

CO line emission in the halo of a radio galaxy at $z=2.6^*$

N. P. H. Nesvadba^{1,2†}, R. Neri³, C. De Breuck⁴, M. D. Lehnert², D. Downes³,
 F. Walter⁵, A. Omont⁶, F. Boulanger¹, N. Seymour⁷

¹*Institut d’Astrophysique Spatiale, Université Paris Sud 11, Orsay, France*

²*GEPI, Observatoire de Paris, CNRS, Université Denis Diderot, Meudon, France*

³*Institut de Radio Astronomie Millimétrique (IRAM), St. Martin d’Heres, France*

⁴*European Southern Observatory, Karl-Schwarzschild Strasse, Garching bei München, Germany*

⁵*Max Planck Institut für Astronomie, Heidelberg, Germany*

⁶*Institut d’Astrophysique de Paris, CNRS, Université Pierre et Marie Curie, Paris*

⁷*Mullard Space Science Laboratory, UCL, Holmbury St. Mary, Dorking, Surrey, RH5 6NT, UK*

30 October 2021

ABSTRACT

We report the detection of luminous CO(3–2) line emission in the halo of the $z=2.6$ radio galaxy (HzRG) TXS0828+193, which has no detected counterpart at optical to mid-infrared wavelengths implying a stellar mass $\lesssim \text{few} \times 10^9 M_\odot$ and relatively low star-formation rates. With the IRAM PdBI we find two CO emission line components at the same position at ~ 80 kpc distance from the HzRG along the axis of the radio jet, with different blueshifts of few 100 km s^{-1} relative to the HzRG and a total luminosity of $\sim 2 \times 10^{10} \text{ K km s}^{-1} \text{ pc}^2$ detected at a total significance of $\sim 8\sigma$. HzRGs have significant galaxy overdensities and extended halos of metal-enriched gas often with embedded clouds or filaments of denser material, and likely trace very massive dark-matter halos. The CO emission may be associated with a gas-rich, low-mass satellite galaxy with very little on-going star formation, in contrast to all previous CO detections of galaxies at similar redshifts. Alternatively, the CO may be related to a gas cloud or filament and perhaps jet-induced gas cooling in the outer halo, somewhat in analogy with extended CO emission found in low-redshift galaxy clusters.

Key words: galaxies: high-redshift, galaxies: individual TXS0828+193, radio lines: galaxies

1 INTRODUCTION

The most vigorous starbursts in the Universe occurred in massive galaxies during the most active phase of galaxy evolution and AGN activity, at redshifts $z \sim 2-3$. These galaxies formed most of their stellar mass of a few $\times 10^{10-11} M_\odot$ in short bursts of few $\times 100$ Myrs with star-formation rates of several $100 M_\odot \text{ yr}^{-1}$ (e.g., Smail et al. 2002; Archibald et al. 2001; Reuland et al. 2004). Luminous CO emission observed at millimeter wavelengths is typically viewed as the most direct sign of the immense reservoirs of cold molecular gas necessary to fuel these starbursts (e.g., Greve et al. 2005).

Powerful high-redshift radio galaxies (HzRGs) may host the most extreme starbursts at high redshift (e.g., Seymour et al. 2008), seen in a short, but critical phase of their evolution dominated by strong AGN feedback (Nesvadba et al. 2006, 2007, 2008). Bright K-band magni-

tudes suggest HzRGs are among the most massive galaxies at all cosmic epochs (e.g., De Breuck et al. 2002), a conclusion recently confirmed through rest-frame near-infrared photometry. Seymour et al. (2007) find stellar masses of several $10^{11} M_\odot$, factors of a few larger than typical masses of submillimeter galaxies at similar redshifts ($10^{10.5} M_\odot$, Smail et al. 2004). Luminous CO emission has been found in several HzRGs (e.g., Papadopoulos et al. 2000; De Breuck et al. 2005; Klamer et al. 2005), and recently also in a satellite galaxy of a HzRG (Ivison et al. 2008).

HzRGs reside in particularly rich environments, and are often surrounded by several 10s of companion galaxies (e.g., Le Fevre et al. 1996; Kurk et al. 2004; Venemans et al. 2007) as well as extended halos of ionized and neutral gas. Faint, diffuse Ly α emission extends to radii well beyond the inner halo, where the gas is strongly disturbed by the radio jet. Villar-Martín et al. (2002, 2003) trace ionized gas out to radii of > 100 kpc with relatively quiescent kinematics and CIV emission line ratios implying near-solar metallicities out to large radii. Deep Ly α absorption troughs reveal neutral gas, likely in clouds or filaments (e.g., van Ojik et al. 1997).

* Based on observations collected at the IRAM Plateau de Bure Interferometer (PdBI).

† E-mail: nicole.nesvadba@ias.u-psud.fr

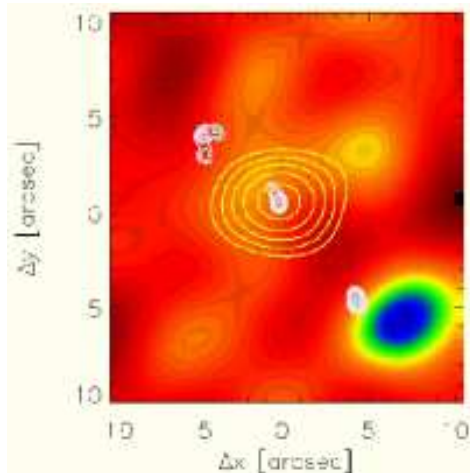


Figure 1. CO(3–2) line image, integrated over the full wavelength range of the two components. Line emission is not spatially resolved with a $5''$ beam. Thick yellow and thin white contours show the non-thermal continuum observed at 3mm with the PdBI and at 8.4 GHz with the VLA, respectively.

Using the IRAM Plateau de Bure Interferometer we detected luminous CO(3–2) line emission in the halo of the $z=2.6$ HzRG TXS0828+193, with a luminosity of 2×10^{10} K km s $^{-1}$ pc 2 . Deep photometry from the rest-frame UV to mid-infrared including MIPS $24\mu\text{m}$ imaging does not reveal a counterpart within the $5''$ beam, implying a very small associated stellar mass and low star-formation rates. These are very unusual properties for a high-redshift CO emitter, and we discuss possible scenarios for its nature. Throughout the paper, we adopt a flat $H_0 = 70$ km s $^{-1}$ Mpc $^{-3}$ concordance cosmology with $\Omega_\Lambda = 0.7$ and $\Omega_M = 0.3$.

2 OBSERVATIONS AND ANCILLARY DATA

We observed TXS0828+193 with the IRAM Plateau de Bure Interferometer PdBI (Guilloteau et al. 1992) in the D configuration. At $z=2.6$, CO(3–2) falls at 96.6 GHz and into the 3 mm atmospheric window. We reached an 0.3 mJy/beam rms and a beam size of $5.3'' \times 4.6''$ (42×37 kpc at $z=2.6$). On-source integration time was 12.9 hrs under normal to good conditions with 6 antennae and system temperatures < 150 K. Data were calibrated using the CLIC package and with MWC349 as flux calibrator. We combined both polarizations and rebinned the data to a resolution of 30 km s $^{-1}$. The PdBI receivers covered a window of ~ 2600 km s $^{-1}$.

We also include deep Palomar WIRC K-band imaging, and SPITZER IRAC $3.6\mu\text{m}$ and MIPS $24\mu\text{m}$ photometry, as well as archival HST WFPC2 F606W imaging. C. Carilli kindly provided his VLA 8.4 GHz A-array map of TXS0828+193 first published in Carilli et al. (1997). We detected the millimeter continuum of the radio core of TXS0828+193. Thus, we could align the PdBI data with our line-free K band continuum image of TXS0828+193 (Nesvadba et al. 2008), assuming that the AGN is at the center of the galaxy. The K band data then served as a reference to align all other images.

3 CO EMISSION IN THE HALO OF A HZRG

We identify luminous CO(3–2) emission in the halo of TXS0828+193 at a distance of $\sim 10''$ (80 kpc) south-west from the radio galaxy (Fig. 1). The $5''$ beam corresponds to an upper size limit of ~ 40 kpc. The emission line region is aligned with the axis of the radio jet but $2.5''$ (20 kpc) WSW in projection from the radio lobe, and hence at a larger radius from the central galaxy. Integrating over the full line we reach 8σ significance. To further ensure the robustness of our measurement, we split the data into two subsamples with consistent results in each subset.

The integrated spectrum is shown in Fig. 2. We find 2 compact components, labeled TXS0828+193 SW1 and SW2, respectively. They have the same spatial position, but different blueshifts of $\Delta v_{\text{SW1}} = -200 \pm 40$ km s $^{-1}$ and $\Delta v_{\text{SW2}} = -920 \pm 70$ km s $^{-1}$ relative to the HzRG, respectively. The systemic velocity was estimated from rest-frame optical integral-field spectroscopy of TXS0828+193 (Nesvadba et al. 2008). SW1 and SW2 have line widths $\text{FWHM}_{\text{SW1}} = 310 \pm 270$ km s $^{-1}$ and $\text{FWHM}_{\text{SW2}} = 340 \pm 270$ km s $^{-1}$, respectively. Integrated fluxes are $I_{\text{CO,SW1}} = 0.23 \pm 0.08$ Jy km s $^{-1}$ and $I_{\text{CO,SW2}} = 0.24 \pm 0.06$ Jy km s $^{-1}$, respectively, and correspond to luminosities of $\mathcal{L}'_{\text{CO}} = 9 \times 10^9$ K km s $^{-1}$ pc 2 per component. (We assumed $\mathcal{L}'_{3-2} = \mathcal{L}'_{1-0}$ and $r_{32} = 1$).

Molecular gas mass estimates of high-redshift galaxies depend on the assumption that the conversion factors from CO to H $_2$ (“X factors”) established at low redshift will apply. The X-factor of $X_U = 0.8 M_\odot / (\text{K km s}^{-1} \text{ pc}^2)$ appropriate for ULIRGs yields estimates $\sim 5 \times$ lower than the Milky Way X-factor (Downes & Solomon 1998). With X_U , the $I_{\text{SW1}} \sim S_{\text{SW2}} \sim 0.25$ Jy km s $^{-1}$ per component correspond to $7 \times 10^9 M_\odot$ in cold gas per component, or $1.4 \times 10^{10} M_\odot$ in total.

We will now discuss two possible scenarios for the nature of the CO emission in the halo of TXS0828+193, namely, that it may be associated with a satellite galaxy, or that it may be related to gas clouds or filaments within the gas-rich halo of TXS0828+193.

3.1 An extremely gas-rich satellite galaxy?

We searched for the stellar continuum of putative galaxies associated with SW1/2 in our set of images with rest-frame wavelengths between $\sim 1700\text{\AA}$ and $7\mu\text{m}$ (§3). SW1/2 was not detected in any of the data sets (Fig. 3). This is in strong contrast to the companion of the $z=3.8$ HzRG 4C60.07, that was detected in all bands in a similar study of Ivison et al. (2008). We use the deep K-band photometry with a 3σ limit of $K_{3\sigma} = 23.7$ mag in a $1''$ aperture and the population synthesis models of Bruzual & Charlot (2003), to place an upper limit on the stellar mass. Continuous star-formation histories with ages between 5×10^7 yrs and 2×10^9 yrs (implying a formation at $z \lesssim 10$), and extinctions $A_V = 1 - 5$ mag correspond to a maximum of $\sim 3 \times 10^9 M_\odot$ in stellar mass. This covers more than the range of extinctions found for dusty submillimeter galaxies at $z \geq 2$ and low-redshift ULIRGs typically associated with strong CO emission ($A_V \lesssim 2$ mag Smail et al. 2004; Scoville et al. 2000). These extinctions are derived from the integrated photometry of the galaxies, as appropriate for our purposes. Extinctions along individual sightlines and into a starburst may be significantly higher.

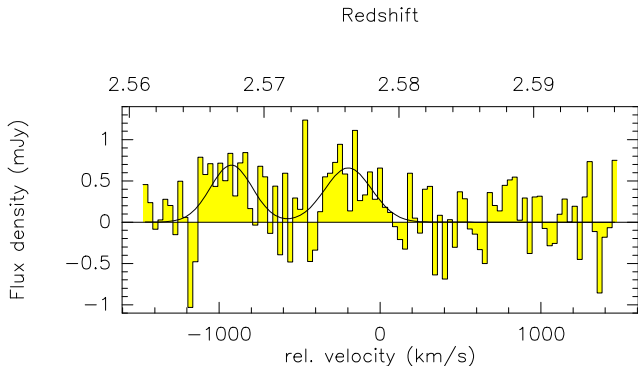


Figure 2. Integrated spectrum of the CO emitter south-west from TXS082+193. The yellow histogram marks the data, with a Gaussian fit of two components overlaid (black line). The blueshifted and redshifted components are detected at 3σ and 4σ significance, respectively.

The r.m.s. of $\sim 100 \mu\text{Jy}$ in our MIPS $24\mu\text{m}$ image is well below the fluxes measured by Pope et al. (2008) for submillimeter galaxies at similar redshifts, which are in the range $200\text{--}500\mu\text{Jy}$. This allows us to set constraints on the star formation, because the filter covers the $6.2\mu\text{m}$ PAH band, and more than half of the $7.7\mu\text{m}$ band at the redshift of SW1/2. With the MIPS non-detection, it appears unlikely that SW1/2 is forming stars at the prodigious rates of several $100 M_{\odot}$ typically observed in SMGs.

We will now estimate a dynamical mass for SW1/2. With a beam size of 40 kpc , we do not know whether the CO line emission may be associated with one or with two galaxies. If SW1/2 represent a double-horned profile of a single, roughly virialized, rotating galaxy (as often assumed for SMGs), we can estimate a mass by setting $M_{\text{dyn}} = (v/\sin i)^2 R_{1\text{kpc}}/G$ with circular velocity $v = 350 \text{ km s}^{-1}$, inclination i , radius $R_{1\text{kpc}}$, and gravitational constant, G . The radius R is given in kpc. Tacconi et al. (2008) use radii $\sim 2\text{--}5 \text{ kpc}$ for their mass estimates, which would imply $M_{\text{dyn}} \sim 0.6 - 1.5 \times 10^{11} M_{\odot}$ for an edge-on disc, and, perhaps more realistically, $2\text{--}3\times$ higher masses for a more average inclination. Thus, SW1/2 would have a mass in the typical range of submillimeter galaxies or powerful radio galaxies, which are $K \sim 20$ mag or brighter (Smail et al. 2004; De Breuck et al. 2002). This would also significantly exceed the baryonic (gas and stellar) mass of $\text{few} \times 10^{10} M_{\odot}$. If alternatively, we assume that SW1 and SW2 are associated with two different galaxies in the halo of TXS0828+193 (a plausible assumption given the 40 kpc covered by the beam), then, following Neri et al. (2003), we estimate a dynamical mass of $M_{\text{dyn}} = 4 \times 10^9 R_{1\text{kpc}} M_{\odot}$ per galaxy for a FWHM= 300 km s^{-1} line width of each component. Assuming a radius of a few kpc, the dynamical mass estimate will be lower than the molecular gas mass by factors of a few, except if we assume that both galaxies are seen within a few degrees from being face-on, which does not appear very likely. Each of these estimates relies on the assumption that the gas is approximately virialized. This is a common assumption in CO emission line studies at high redshift, but whether it is justified has yet to be proven. In §3.2 we discuss a scenario where the virial assumption would not apply. Likewise Ivison et al. (2008) raised doubts as to whether this

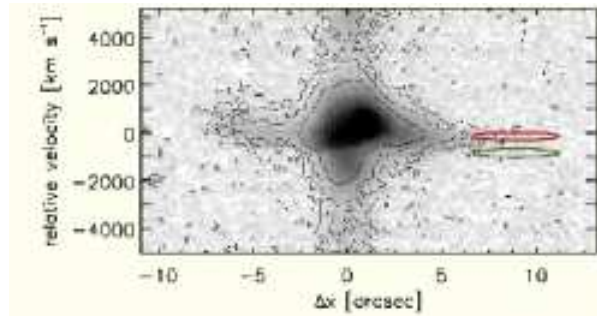


Figure 4. Ly α spectrum of TXS0828+193, graciously provided by M. Villar-Martin with the CO(3–2) components SW1 and SW2 shown as red and green ellipses, respectively. Positions and sizes correspond to the distance from the HzRG and beam size, and to the relative redshift and FWHM line width of the two components, respectively.

assumption is always justified in the context of high-redshift galaxies.

In these “galaxy” scenarios, we also need a mechanism to suppress star formation in the cold gas traced by the CO. If the CO line emission arises from a disc with a few kpc in radius, then the observed gas mass of $1.4 \times 10^{10} M_{\odot}$ corresponds to a surface mass density of $\text{few} \times 1000 M_{\odot} \text{ pc}^{-2}$. Following the Schmidt-Kennicutt relation (Kennicutt 1998) between gas surface density and star formation intensity, SFI, we expect $\text{SFI} = \text{few} \times 10 M_{\odot} \text{ yr}^{-1} \text{ kpc}^{-2}$. Averaging over the size of the disc, this corresponds to a total star-formation rate of several $100 M_{\odot} \text{ yr}^{-1}$. This is in the typical range of submillimeter galaxies, but in contradiction with our non-detection at $24\mu\text{m}$. Likewise, with star-formation rates of $\text{few} \times 100 M_{\odot} \text{ yr}^{-1}$ a stellar mass of $\text{few} \times 10^9 M_{\odot}$ would be built in $\text{few} \times 10^7$ yrs, so that SW1/2 would have to be in a very special, very young stage of the starburst if it was a galaxy.

Papadopoulos et al. (2008) recently found luminous, but excited CO line emission in a nearby radio galaxy, 3C293, which does not seem associated with a starburst. The same is suggested by Spitzer observations of a small number of nearby galaxies with strongly enhanced, mid-infrared H_2 line emission (e.g., Ogle et al. 2007). Guillard et al. (2009) argue that this gas may be heated through the dissipation of kinetic energy. In these cases, it is likely that the energy was injected by an external mechanism (a merger or AGN). We will in the following propose a somewhat related scenario, where the nearby radio lobe may have induced the collapse of gas within the halo of TXS0828+193.

3.2 Cold gas in the halo?

TXS0828+193 was the first HzRG where an outer halo was found (Villar-Martín et al. 2002), which extends beyond the turbulent, luminous inner emission line region that is likely powered by energy released from the powerful AGN (e.g., Villar-Martín et al. 1999; Nesvadba et al. 2008). Diffuse gas in the outer halo is fainter, and has more moderate velocity gradients and line widths, which may indicate rotation in the potential of the underlying dark-matter halo (Villar-Martín et al. 2003, 2006), or perhaps gas inflow (Humphrey et al. 2007). Villar-Martín et al. (2002) find

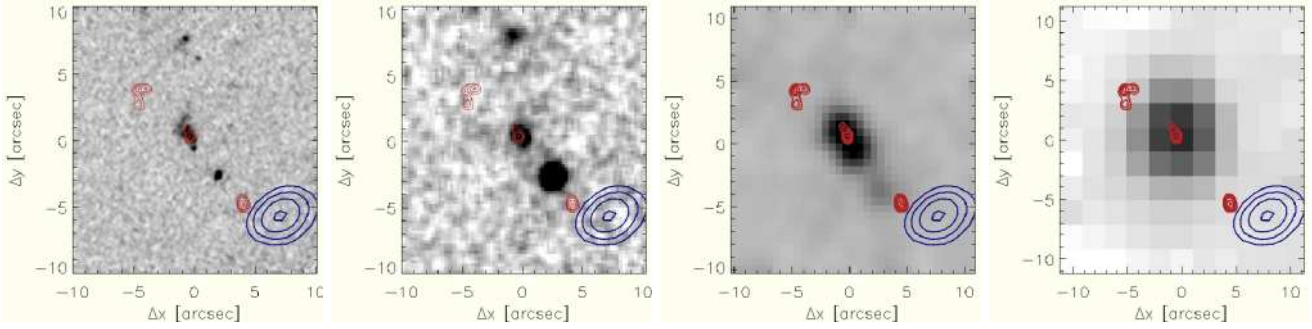


Figure 3. (left to right:) HST WFPC606W, Palomar K band, Spitzer IRAC 3.6 μ m and MIPS 24 μ m photometry of TXS0828+193. Thick blue contours show the position of the SW1/SW2, thin red contours mark radio jets. SW1/SW2 is undetected in all bands.

CIV emission in the outer halo of TXS0828+193 and suspect that metallicities may be up to nearly solar, perhaps representing gas that has previously been driven out from the central galaxy.

Fig. 4 shows the relative velocity and radial distance of SW1 and SW2 from TXS0828+193 relative to the two-dimensional Ly α longslit spectrum of Villar-Martín et al. (2002). The slit of the Ly α spectrum falls near the CO position, but since the slit width, 1'', is significantly smaller than the beam of 5'', we cannot infer whether it covers the position of the CO emitter. Ly α emission is traced almost out to the 24 kpc radial distance of SW1/2 from the HzRG.

SW1 and SW2 are blueshifted relative to the radio galaxy, and are also on the side of the radio galaxy where the diffuse Ly α halo is blueshifted (the luminous inner halo is redshifted). The kinematic properties of SW1 (FWHM=310 \pm 270 km s $^{-1}$, $z=2.5761\pm 0.0008$) are very similar to those of the diffuse ionized gas (FWHM=590 \pm 60 km s $^{-1}$, $z=2.5741\pm 0.0008$), with a relative blueshift of SW1 relative to the Ly α emission of 170 \pm 60 km s $^{-1}$. SW2 (FWHM= 340 \pm 270, $z=2.5678\pm 0.0007$) is blueshifted by 890 km s $^{-1}$ relative to the diffuse Ly α emission, but has a similar line width within large uncertainties. Given the low stellar mass possibly associated with the CO line emission (§ 3.1), this may suggest that the CO emission originates from clouds or filaments in the diffuse halo gas of TXS0828+193, which has metallicities of up to about solar (Villar-Martín et al. 2002). De Breuck et al. (2003) detected CO emission at the redshift of a Ly α absorber near the $z=3.1$ HzRG B2 2330+3927, and proposed a similar scenario, but did not have the spatial resolution to directly measure positional offsets between the radio galaxy and CO emission.

Several mechanisms may plausibly influence the halo gas including minor or major mergers, or powerful outflows from starbursts and AGN. Each of these mechanisms may sweep up and accelerate halo gas over timescales of a few $\times 10^8$ yrs similar to those suggested by the relative velocity of the CO and distance to the radio galaxy. The close proximity of the emitters to the radio hot spot and alignment with the jet axis is however suspicious. The emitters are very close to the jet axis, and within a projected area of ~ 300 kpc 2 from the hot spot, whereas our data have a half-power beam width covering a total of 135,000 kpc 2 . If this is not due to mere projection effects, then weak shocks produced by the expanding radio source may play a role in compressing and exciting the gas (the radio hot spot is only about 2.5'' or 20

kpc away, and we may not detect the low surface brightness radio plasma). In turn, the interaction with dense gas may be enhancing or even triggering the radio hot spot.

Extended cold molecular gas is found in some massive cooling-flow clusters at low redshift (e.g., Edge 2001; Salomé & Combes 2004), where molecular gas forms along the edges of X-ray cavities inflated by the radio jet and outside the volume filled by the radio plasma. Similarly, CO line emission in the halos of HzRGs may trace the edges of cavities inflated by the radio lobes. Within the large uncertainties, the ~ 300 km s $^{-1}$ FWHM of SW1/2 are not very different from the line widths in the diffuse CO in the Perseus cluster (Salomé et al. 2008).

We can use the observed surface brightness of the faint Ly α emission in the halo of TXS0828+193 and the observed CO luminosity to investigate whether TXS0828+193 falls near the correlation between the luminosity of the molecular and ionized gas found in local cooling-flow clusters (Edge 2001). Adopting a flux conversion $\mathcal{L}_{Ly\alpha} = 13 \times \mathcal{L}_{H\alpha}$ between Ly α and H α luminosity (where we neglect extinction), we find a strict upper limit on the Ly α luminosity of $\mathcal{L}_{Ly\alpha} = 1.4 \times 10^{42}$ erg s $^{-1}$ cm $^{-2}$ within the 20'' area of the beam. Translating the CO gas mass of Edge (2001) into a CO luminosity, we find that the halo of TXS0828+193 falls only factors of a few below the expected value found in local cooling-flow clusters. Allowing for different physical conditions, gas distributions, and AGN properties (HzRGs host powerful AGN), we may well be seeing a fundamentally similar phenomenon.

However, the brightness temperatures and spatial distribution of the extended CO emission in low-redshift clusters are significantly different. Low brightness temperatures suggest low gas filling factors, and much of the gas is concentrated towards the central radio galaxy. This may arise from different properties of the diffuse cluster gas at high and low redshift, which is cold for HzRGs (with embedded filaments or clouds of few $\times 10^9$ M $_{\odot}$ and more in dense neutral gas van Ojik et al. 1997) and hot and rarefied in low-redshift clusters. In fact, in HzRGs at $z \sim 2-3$ we may be witnessing the processes that led to the rapid heating and entropy enhancement of cluster gas through AGN feedback, which seem necessary to explain the temperature profiles of massive X-ray clusters at low redshift (Nath & Roychowdhury 2002; McCarthy et al. 2008). Interestingly, Ly α absorbers are only found in the halos of HzRGs with relatively small, and likely rather young, radio sources. This suggests that

large amounts of dense gas (and perhaps dust) may be present in the halo at radii that are not yet affected by mechanical heating from the radio source. The approaching radio jet of TXS0828+193 may have contributed to triggering the collapse and forming SW1/2. Similar processes may ultimately lead to positive AGN feedback and jet-triggered star formation in some cases, if the cold molecular gas will relax and form stars over sufficiently short time scales.

4 SUMMARY AND CONCLUSIONS

We discuss the nature of luminous CO(3–2) line emission in the halo of the radio galaxy TXS0828+193 at $z=2.6$. The CO emission resembles that of submillimeter galaxies, but we do not detect continuum emission from SW1/2, including $24\mu\text{m}$ MIPS imaging, which covers the PAH bands at $z=2.6$. For a gas disc in a galaxy we would expect strong star formation if the Schmidt-Kennicutt law roughly applies.

Alternatively, SW1/2 may represent a cloud or filament in the halo, maybe related to neutral, dense Ly α absorbers observed near some HzRGs. The approaching radio jet of TXS0828+193 may have contributed to triggering the collapse and exciting the gas. This is somewhat in analogy with diffuse CO emission in low-redshift clusters, but the ambient gas properties will likely be very different at $z=2.6$. In either case, SW1/2 does not appear to be an 'ordinary' high-redshift CO emitter, and further observations are necessary to differentiate between the two scenarios. This suggests that CO observations of the high-redshift Universe with the refurbished PdBI and soon with ALMA, will reveal a rich, and multi-faceted picture of the early Universe.

ACKNOWLEDGMENTS

We would like to thank the staff at IRAM for carrying out the observations and for hospitality during the data reduction. We also thank M. Villar-Martín and C. Carilli for valuable discussion and for generously sharing their data. NPHN thanks P. Salomé, G. Bicknell, and M. Krause for interesting discussions. We thank the referee for comments which helped improve the paper. NPHN acknowledges financial support through a fellowship of the Centre National d'Etudes Spatiales (CNES) and through a Marie Curie Fellowship of the European Commission. IRAM is funded by the Centre National de Recherche Scientifique, the Max-Planck Gesellschaft and the Instituto Geografico Nacional.

REFERENCES

- Archibald E. N., Dunlop J. S., Hughes D. H., Rawlings S., Eales S. A., Ivison R. J., 2001, *MNRAS*, 323, 417
 Bruzual G., Charlot S., 2003, *MNRAS*, 344, 1000
 Carilli C. L., Roettgering H. J. A., van Ojik R., Miley G. K., van Breugel W. J. M., 1997, *ApJS*, 109, 1
 De Breuck C., Downes D., Neri R., van Breugel W., Reuland M., Omont A., Ivison R., 2005, *A&A*, 430, L1
 De Breuck C., Neri R., Morganti R., Omont A., Rocca-Volmerange B., Stern D., Reuland M., van Breugel W., Röttgering H., Stanford S. A., Spinrad H., Vigotti M., Wright M., 2003, *A&A*, 401, 911
 De Breuck C., van Breugel W., Stanford S. A., Röttgering H., Miley G., Stern D., 2002, *AJ*, 123, 637
 Downes D., Solomon P. M., 1998, *ApJ*, 507, 615
 Edge A. C., 2001, *MNRAS*, 328, 762
 Greve T. R., Bertoldi F., Smail I., Neri R., Chapman S. C., Blain A. W., Ivison R. J., Genzel R., Omont A., Cox P., Tacconi L., Kneib J.-P., 2005, *MNRAS*, 359, 1165
 Guillard P., Boulanger F., Pineau de Forets G., et al., 2009, *A&A* submitted
 Guilloteau S., Delannoy J., Downes D., Greve A., Guelin M., Lucas R., Morris D., Radford S. J. E., Wink J., Cernicharo J., Forveille T., Garcia-Burillo S., Neri R., Blondel J., Perrigourad A., Plathner D., Torres M., 1992, *A&A*, 262, 624
 Humphrey A., Villar-Martín M., Fosbury R., Binette L., Vernet J., De Breuck C., di Serego Alighieri S., 2007, *MNRAS*, 375, 705
 Ivison R. J., Morrison G. E., Biggs A. D., Smail I., Willner S. P., Gurwell M. A., Greve T. R., Stevens J. A., Ashby M. L. N., 2008, *MNRAS*, 390, 1117
 Kennicutt Jr. R. C., 1998, *ApJ*, 498, 541
 Klamer I. J., Ekers R. D., Sadler E. M., Weiss A., Hunstead R. W., De Breuck C., 2005, *ApJ*, 621, L1
 Kurk J. D., Pentericci L., Overzier R. A., Röttgering H. J. A., Miley G. K., 2004, *A&A*, 428, 817
 Le Fevre O., Deltorn J. M., Crampton D., Dickinson M., 1996, *ApJ*, 471, L11+
 McCarthy I. G., Babul A., Bower R. G., Balogh M. L., 2008, *MNRAS*, 386, 1309
 Nath B. B., Roychowdhury S., 2002, *MNRAS*, 333, 145
 Neri R., Genzel R., Ivison R. J., Bertoldi F., Blain A. W., Chapman S. C., Cox P., Greve T. R., Omont A., Frayer D. T., 2003, *ApJ*, 597, L113
 Nesvadba N. P. H., Lehnert M. D., De Breuck C., Gilbert A., van Breugel W., 2007, *A&A*, 475, 145
 Nesvadba N. P. H., Lehnert M. D., De Breuck C., Gilbert A. M., van Breugel W., 2008, *A&A*, 491, 407
 Nesvadba N. P. H., Lehnert M. D., Eisenhauer F., Gilbert A., Tecza M., Abuter R., 2006, *ApJ*, 650, 693
 Ogle P. M., Antonucci R., Appleton P. N., Boulanger F., Evans A., Emonts B. H. C., Whysong D., 2007, in *Bulletin of the American Astronomical Society Vol. 38 of Bulletin of the American Astronomical Society, Molecular Hydrogen Emission Galaxies*. pp 907–+
 Papadopoulos P. P., Kovacs A., Evans A. S., Barthel P., 2008, *A&A*, 491, 483
 Papadopoulos P. P., Röttgering H. J. A., van der Werf P. P., Guilloteau S., Omont A., van Breugel W. J. M., Tilanus R. P. J., 2000, *ApJ*, 528, 626
 Pope A., Chary R.-R., Alexander D. M., Armus L., Dickinson M., Elbaz D., Frayer D., Scott D., Teplitz H., 2008, *ApJ*, 675, 1171
 Reuland M., Röttgering H., van Breugel W., De Breuck C., 2004, *MNRAS*, 353, 377
 Salomé P., Combes F., 2004, *A&A*, 415, L1
 Salomé P., Combes F., Revaz Y., Edge A. C., Hatch N. A., Fabian A. C., Johnstone R. M., 2008, *A&A*, 484, 317
 Scoville N. Z., Evans A. S., Thompson R., Rieke M., Hines D. C., Low F. J., Dinshaw N., Surace J. A., Armus L., 2000, *AJ*, 119, 991
 Seymour N., Ogle P., De Breuck C., Fazio G. G., Galametz A., Haas M., Lacy M., Sajina A., Stern D., Willner S. P.,

- Vernet J., 2008, *ApJ*, 681, L1
- Seymour N., Stern D., De Breuck C., Vernet J., Rettura A., Dickinson M., Dey A., Eisenhardt P., et al., 2007, *ApJS*, 171, 353
- Smail I., Chapman S. C., Blain A. W., Ivison R. J., 2004, *ApJ*, 616, 71
- Smail I., Ivison R. J., Blain A. W., Kneib J.-P., 2002, *MNRAS*, 331, 495
- Tacconi L. J., Genzel R., Smail I., Neri R., Chapman S. C., Ivison R. J., Blain A., Cox P., et al., 2008, *ApJ*, 680, 246
- van Ojik R., Roettgering H. J. A., Miley G. K., Hunstead R. W., 1997, *A&A*, 317, 358
- Venemans B. P., Röttgering H. J. A., Miley G. K., van Breugel W. J. M., de Breuck C., Kurk J. D., Pentericci L., Stanford S. A., Overzier R. A., Croft S., Ford H., 2007, *A&A*, 461, 823
- Villar-Martín M., Sánchez S. F., De Breuck C., Peletier R., Vernet J., Rettura A., Seymour N., Humphrey A., Stern D., di Serego Alighieri S., Fosbury R., 2006, *MNRAS*, 366, L1
- Villar-Martín M., Tadhunter C., Morganti R., Axon D., Koekemoer A., 1999, *MNRAS*, 307, 24
- Villar-Martín M., Vernet J., di Serego Alighieri S., Fosbury R., Humphrey A., Pentericci L., 2003, *MNRAS*, 346, 273
- Villar-Martín M., Vernet J., di Serego Alighieri S., Fosbury R., Pentericci L., Cohen M., Goodrich R., Humphrey A., 2002, *MNRAS*, 336, 436